

Short Communication

## Hydrothermal Synthesis of $\alpha$ -MoO<sub>3</sub> and the Influence of Later Heat Treatment on its Electrochemical Properties

Yan Wang<sup>1</sup>, Yongchun Zhu<sup>1</sup>, Zheng Xing<sup>1</sup>, and Yitai Qian<sup>1,2,\*</sup>

<sup>1</sup> Hefei National Laboratory for Physical Sciences at Microscale and Department of Chemistry, University of Science and Technology of China, Hefei, Anhui, 230026, P. R. China.

<sup>2</sup> School of Chemistry and Chemical Engineering, Shandong University, Jinan, 250100, P. R. China

\*E-mail: [ytqian@ustc.edu.cn](mailto:ytqian@ustc.edu.cn)

Received: 13 May 2013 / Accepted: 5 June 2013 / Published: 1 July 2013

---

$\alpha$ -MoO<sub>3</sub> nanorods were obtained by hydrothermal method. The influence of later heat treatment on its electrochemical properties was also investigated. In the electrochemical measurements, the annealed  $\alpha$ -MoO<sub>3</sub> nanorods exhibited better performance than the hydrothermal gained ones. It is proposed that the strong chemical bonds in the annealed product contribute to the good cycling stability.

---

**Keywords:** Molybdenum oxide; Hydrothermal synthesis; Later heat treatment; electrochemical properties

### 1. INTRODUCTION

As the energy problem becomes more and more severe, lithium ion battery receive special attention these days. Its potential use in electric or hybrid electric vehicles encourages intensive study to improve the performances, such as high energy density, good cycling stability, long operating time, etc.[1] Among all the researches on lithium ion battery at present, the electrode materials received a particular attention. Numerous great efforts are made to seek appropriate electrode materials which can provide superior function.[2] In particular, transition metal oxides including ferric oxide, cobalt oxide, copper oxide, nickel oxide, and molybdenum oxide are likely to be classical electrode materials fabricated in lithium ion battery.[3]

Molybdenum trioxide (MoO<sub>3</sub>) is one of the most interesting transition metal oxides due to its unique layered structure and distinctive electrochemical property.[4] There are three basic polytypes of MoO<sub>3</sub>. The thermodynamically stable orthorhombic MoO<sub>3</sub> ( $\alpha$ -type)[5], metastable monoclinic MoO<sub>3</sub> ( $\beta$ -type)[6], and hexagonal MoO<sub>3</sub> (h-type)[7], among which  $\alpha$ -MoO<sub>3</sub> is the most important form. In  $\alpha$ -

MoO<sub>3</sub>, the molybdenum atoms coordinate six oxygen atoms to form MoO<sub>6</sub> octahedra, which connected by edge sharing along [001] direction to form a zigzag chain. The chains are mutually interlinked with their corners along [100] direction, resulting in a double-layer sheet, which propagate along [010] direction via der Waals interactions to form the layered structure of  $\alpha$ -MoO<sub>3</sub>. [3]

Over the past decades, many researches have been made to prepare  $\alpha$ -MoO<sub>3</sub> via various procedures, such as sol-gel method [8], hydrothermal/solvothermal method [4,9,10], self-propagating combustion [11], flame synthesis technique [12], vapor phase deposition method [13], flash evaporation technique [14], and so on. Different forms of 1-D  $\alpha$ -MoO<sub>3</sub> were obtained, like nanowires [15], nanotubes [16], nanobelts [17,18], and nanorods [19,21]. However, few researches focused on the electrochemical property of  $\alpha$ -MoO<sub>3</sub> and its usage in lithium ion batteries. [19-26] Campanella proposed the concept of using MoO<sub>3</sub> as the electrode material in nonaqueous second battery in 1971, which showed low polarization and good reversibility. [25] In the year 1974, Margalit studied the behavior of Li/MoO<sub>3</sub> cell, as well as its electrode reaction. [26] Whittingham came up with the role of the ternary phase during the electrode reaction. The reversibility should be preferable as long as no chemical bonds were broken under charge/discharge. [28] The question of  $\alpha$ -MoO<sub>3</sub> has been put on hold for a long period until recent years. Dewangan synthesized  $\alpha$ -MoO<sub>3</sub> nanofibers with rapid hydrothermal method, and got desirable electrochemical properties. [31] Shakir discussed the effect of different synthesis temperature of  $\alpha$ -MoO<sub>3</sub> on its electrochemical property. [21] Hashem [29], Mai [30], and Lee [24] worked on the influence of lithium ion insertion in  $\alpha$ -MoO<sub>3</sub> which dramatically improved the cycling capability of the battery. Among these researches focusing on the electrochemical properties of  $\alpha$ -MoO<sub>3</sub>, the impact of annealing was seldom involved.

In this work, high-quality crystalline  $\alpha$ -MoO<sub>3</sub> nanorods were synthesized via a simple hydrothermal method without employing any catalysts or surfactants. Then the as-formed  $\alpha$ -MoO<sub>3</sub> nanorods were annealed in air for a short time. Through the processing, the electrochemical properties of the  $\alpha$ -MoO<sub>3</sub> nanorods were greatly enhanced.

## 2. EXPERIMENTAL

### 2.1. Materials Preparation

The  $\alpha$ -MoO<sub>3</sub> nanorods were synthesized via hydrothermal method. All reagents used in this work were analytical grade, and purchased from Sinopharm Chemical Reagent Co., Ltd without further purification. 10 mmol sodium molybdate (Na<sub>2</sub>MoO<sub>4</sub>·2H<sub>2</sub>O) was dissolved in 43 ml distilled water. Then 2 ml hydrochloric acid was slowly dropwise added to the solution previously gotten with continuously stirring. The as-obtained clear faint yellow solution was transferred into a Teflon-lined stainless autoclave (60 ml capacity), sealed, and kept at 120 °C for 18 h, then air cooled to room temperature naturally. The solid product was filtered off, washed with deionized water and ethanol, and vacuum-dried at 60 °C overnight (sample 1). After drying, the product was annealed at 500 °C in air for 2 h (sample 2).

## 2.2. Materials Characterization

The crystal structure information of the samples was recorded on a Philips X'pert X-ray diffractometer with Cu K $\alpha$  radiation ( $\lambda=1.54182$  Å). The morphology investigations were characterized with Field-emitting scanning electron microscope (FESEM; JEOL-JSM-6700F). High-resolution transmission electron microscope (HRTEM) and selected area electron diffraction (SAED) images were collected with JEOL-2010 with an accelerating voltage of 200 kV. Raman spectra were recorded on a Jobin Yvon (France) LABRAM-HR confocal laser micro-Raman spectrometer at room temperature.

## 2.3. Electrode fabrication and electrochemical measurements

The composite electrodes were prepared via mixing 80 wt% active material, 10 wt% carbon black and 10 wt% polyvinylidene fluoride solution in N-methylpyrrolidone, which were coated onto a copper foil with a diameter of 12 mm as a current collector. The electrolyte was the solution of 1 M LiPF<sub>6</sub> in a mixture of ethylene carbonate (EC) and diethyl carbonate (DEC) with the volume ratio of 1:1. The electrodes were dried at 100 °C in a vacuum furnace for 10 h before use. The cells (CR2016 coin type) were assembled in an argon-filled glove box (Mikrouna, Super 1220/750, China). The electrochemical properties of these cells were measured using the Land battery measurement system (Wuhan, China) at various rates between 0.05 and 3.0 V (versus Li/Li<sup>+</sup>) at room temperature.

## 3. RESULTS AND DISCUSSION

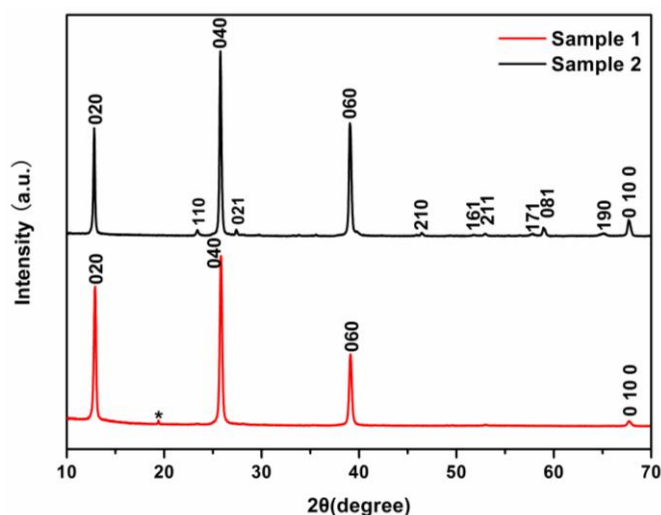


**Figure 1.** XRD patterns of the synthesized  $\alpha$ -MoO<sub>3</sub> nanorods.

The X-ray diffraction patterns of the as-synthesized  $\alpha$ -MoO<sub>3</sub> are shown in Fig. 1. The peaks at 12.8, 25.8, 39.0 and 67.7° in the XRD patterns of both sample 1 and sample 2 are dominant, which could be indexed to (020), (040), and (0 10 0) reflections of orthorhombic  $\alpha$ -MoO<sub>3</sub> with lattice

parameters of  $a = 3.962 \text{ \AA}$ ,  $b = 13.85 \text{ \AA}$  and  $c = 3.697 \text{ \AA}$  (JCPDS Card No. 05-0508). The preferentially orientation of (010) planes suggests that the obtained  $\alpha\text{-MoO}_3$  products should possess a 1-D structure. But the intensity of the reflection peaks are much more ascendent in the XRD pattern of sample 1, indicating that the  $\alpha\text{-MoO}_3$  nanorods in sample 2 are shorter than those in sample 1. The SEM images of the samples (Fig. 2) coincides with the presume. The products obtained after the simple hydrothermal process are nanorods with about 200 nm in radius and 3  $\mu\text{m}$  in length (Fig. 2a). After annealing, the radius of the nanorods broadened to about 500 nm and the length shortened remarkably to 1~2  $\mu\text{m}$  (Fig. 2b). We also observed that there is a little  $\text{H}_6\text{Mo}_{5.35}\text{O}_{19.05}$  (JCPDS Card No. 47-0872) impurity (marked as \* in Fig. 1) in the XRD patterns of sample 1, which disappeared after the heat treatment. It might because the Mo-OH or Mo-(OH)<sub>2</sub> bonds broke during the annealing course, and the element of H and extra O left  $\text{H}_6\text{Mo}_{5.35}\text{O}_{19.05}$  in the form of  $\text{H}_2\text{O}$ . [32]

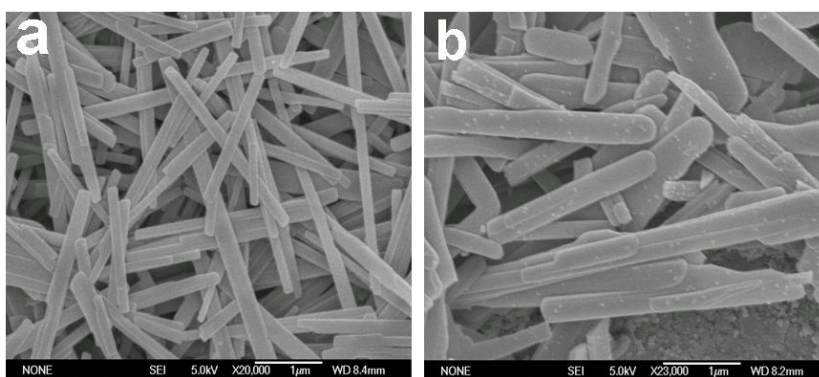


**Figure 2.** SEM images of the synthesized  $\alpha\text{-MoO}_3$  nanorods

The HRTEM image and the corresponding SAED pattern recorded from the nanorod edge of the  $\alpha\text{-MoO}_3$  nanorods obtained through hydrothermal method is shown in Fig. 3a and b, respectively. The measured spacings of the lattice planes are 0.39 and 0.37 nm respectively, which are consistent with the separations of (100) planes and (001) planes of  $\alpha\text{-MoO}_3$ . The selected SAED pattern taken along  $\langle 010 \rangle$  zone axis reveals the single-crystalline nature of the sample.

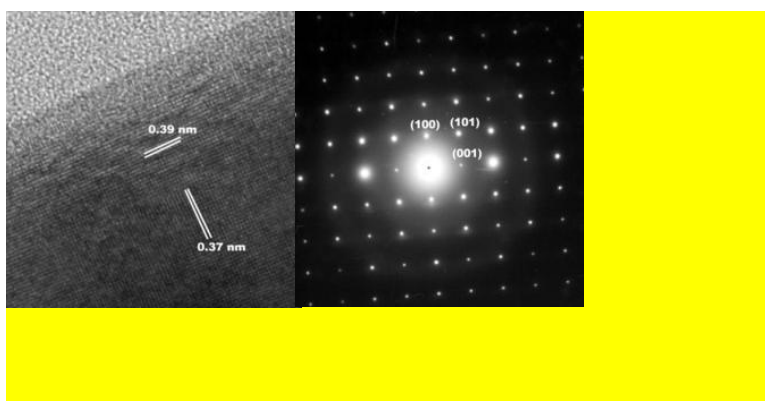


**Figure 3.** HRTEM image and the corresponding SAED pattern of  $\alpha\text{-MoO}_3$

Figure 4a-b illustrates the electrochemical behaviors of the two samples at  $25 \text{ mA g}^{-1}$  between 0.005 and 3.0 V. Figure 4a displays the discharge curves of the two samples during the first cycle. At the end of the first discharge, the discharge capacity of sample 1 ( $1357 \text{ mAh g}^{-1}$ ) is almost the same as that of sample 2 ( $1409 \text{ mAh g}^{-1}$ ). As the charge/discharge cycles continued, the discharge capacity of sample 1 decayed rapidly. The discharge capacity of sample 1 reduced to less than  $100 \text{ mAh g}^{-1}$  after 20 cycles. However, the discharge capacity of sample 2 remained almost the same, and hold a discharge capacity above  $500 \text{ mAh g}^{-1}$  after 20 cycles (Figure 4b). Afterward, the discharge capacity of sample 2 drops steadily, and remained about  $450 \text{ mAh g}^{-1}$  after 90 cycles (Figure 4c). It is thus evident that sample 2, which endured an annealing progress, demonstrates a better cycling stability.

The difference in cycling stability between sample 1 and 2 could be attribute to the poor crystallinity and the presence of appreciable amount of water (as in  $\text{H}_6\text{Mo}_{5.35}\text{O}_{19.05}$ ) within sample 1. [33] During the heat treatment, the water in the sample could be gasified and released effectively. The crystallinity of the sample was improved at the same time. It is reported that the heat treatment could reduce the shear strengths of the sample.[34,35] The Raman spectra of the two samples were recorded. It could be seen from Figure 4d that the Raman intensity of sample 2 is much stronger than the Raman intensity of sample 1. This phenomenon reveals that the chemical bonds, which keep the atoms together, in sample 2 are more powerful. Here, it could be proposed that because of the strong chemical bonds, the atoms of the sample are held together more tightly. Thus the structure of the annealed product (sample 2) could keep unchanged during the lithium ion inert/exert reaction. Therefore, the annealed product gained a good stability during the electrochemical cycles.

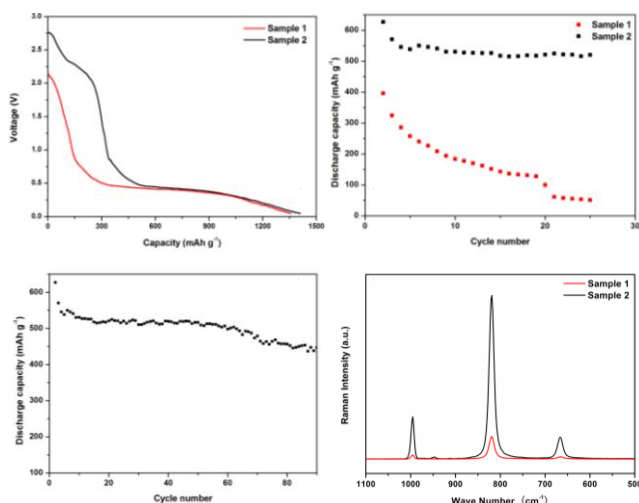


**Figure 4.** (a) The first galvanostatic discharge curve and charge-discharge curves of Sample 1 and 2; (b) Cycling performance of Sample 1 and 2 in 25 cycles; (c) Cycling performance of Sample 2 in 90 cycles; (d) Raman spectra of Sample 1 and 2.

#### 4. CONCLUSION

We have obtained  $\alpha$ -MoO<sub>3</sub> nanorods by hydrothermal method and studied the influence of later heat treatment of the as-synthesized sample on its electrochemical properties. In the electrochemical measurements, the annealed  $\alpha$ -MoO<sub>3</sub> nanorods exhibited better performance than the hydrothermal gained ones. This could be attributed to the crystallinity improvement and water removal during the heat treatment. The stronger chemical bonds in the annealed product could hold the atoms more tightly to keep the structure stable during the electrochemical cycles.

#### ACKNOWLEDGEMENT

This work is financially supported by the National Natural Science Fund of China (no. 91022033, 21171158), the 973 Project of China (no. 2011CB935901).

#### References

1. P. J. Hagrman, D. Hagrman, J. Zubieta, *Angew. Chem., Int. Ed.*, 38 (1999) 2638
2. M. R. Montney, R. L. LaDuca, *J. Solid State Chem.*, 181 (2008) 828
3. J. Zhou, N.S. Xu, S.Z. Deng, J. Chen, J.C. She, Z.L. Wang, *Adv. Mater.*, 15 (2003) 1835.
4. Xiongwen Lou and Huachun Zeng, *Chem. Mater.*, 14 (2002) 4781
5. G. Anderson and A. Magneli, *Acta Chem. Scand.*, 4 (1950) 793
6. E. M. McCarron III, *J. Chem. Soc., Chem. Commun.* (1986), 336
7. N. Sotani, *Bull. Chem. Soc. Jpn.*, 48 (1975) 1820
8. W. Dong and B. Dunn, *Journal of Non-Crystalline Solids*, 225 (1998) 135
9. X. L. Li, J. F. Liu, and Y. D. Li, *Appl. Phys. Lett.*, 81 (2002) 4832
10. G. R. Patzke, A. Michailovski, F. Krumeich, R. d Nesper, J. D. Grunwaldt, and A. Baiker, *Chem. Mater.*, 16 (2004) 1126
11. A. Lagashetty, V. Havanoor, S Basavaraja and A Venkataraman. *Bull. Mater. Sci.*, 28 (2005) 477
12. L. L. Cai, P. M. Rao, and X. L. Zheng, *Nano. Lett.*, 11 (2011) 872
13. H. C. Zeng, *Inorg. Chem.* 1998, 37, 1967
14. C. Julien, A. Khelifa, O. M. Hussain, G. A. Nazri, *Journal of Crystal Growth* 1995, 156, 235
15. Jun Zhou, S. Z. Deng, N. S. Xu, Jun Chen, and J. C. She, *Appl. Phys. Lett.*, 2003, 29, 2653
16. S. Hu and X. Wang, *J. Am. Chem. Soc.*, 130 (2008) 8126
17. T. Xia, Q. Li, X. D. Liu, J. Meng, and X. Q. Cao, *J. Phys. Chem. B*, 110 (2006) 2006
18. X. F. Yang, H. Tang, R. X. Zhang, H. J. Song, and K. S. Cao, *Cryst. Res. Technol.*, 46 (2010) 409
19. J. S. Chen, Y. L. Cheah, S. Madhavi, and X. W. Lou, *J. Phys. Chem. C*, 114 (2010) 8675
20. F. Leroux, L. F. Nazar, *Solid State Ionics*, 133 (2000) 37
21. I. Shakir, M. Shahid, H. W. Yang, D. J. Kang, *Electrochimica Acta*, 56 (2010) 376
22. C. V. S. Teddy, E. H. Walker Jr., C. Wen, S. Mho, *Journal of Power Sources*, 183 (2008) 330
23. L. Q. Mai, F. Yang, Y. L. Zhao, X. Xu, L. Xu, B. Hu, Y. Z. Luo, and H. Y. Liu, *Materials Today*, 14 (2011) 346
24. S. H. Lee, Y. H. Kim, R. Deshpande, P. A. Parilla, E. Whitney, D.T. Gillaspie, K.M. Jones, A. H. Mahan, S. B. Zhang, and A. C. Dillon, *Adv. Mater.*, 20 (2008) 3627
25. L. Campanella and G. Pistoia, *J. Electrochem. Soc.*, 118 (1971) 1905
26. N. Margalit, *Journal of the Electrochemical Society*, 121 (1974) 1460
27. L. Zhou, L. C. Yang, P. Yuan, J. Zou, Y. P. Wu, and C. Z. Yu, *J. Phys. Chem. C*, 114 (2010) 21868
28. M. S. Whittingham, *J. Electrochem. Soc.*, 123 (1976) 315

29. A. M. Hashem, M. H. Askar, M. Winter, J. H. Albering, and J. O. Besenhard, *Ionics*, 13 (2007) 3
30. L. Q. Mai, B. Hu, Y. Y. Qi, Y. Dai, W. Chen, *Int. J. Electrochem. Sci.*, 3 (2008) 216
31. K. Dewangan, N. N. Sinha, P. K. Sharma, A. C. Pandey, N. Munichandraiah, and N. S. Gajbhiye, *CrystEngComm*, 13 (2011) 927
32. H. J. Lunk, H. Hartl, M. A. Hartl, M. J. G. Fait, I. G. Shenderovich, M. Feist, T. A. Frisk, L. L. Daemen, D. Mauder, R. Eckelt, and A. A. Gurinov, *Inorg. Chem.*, 49 (2010) 9400
33. Z. Y. Wang, D. Y. Luan, F. Y. C. Boey, and X. W. Lou, *J. Am. Chem. Soc.*, 133 (2011) 4738
34. M. Yadegari, A. R. Ebrahimi and A. Karami, *Materials Science and Technology*, 29 (2013) 69
35. I. K. Kim, S. I. Hong, *Materials and Design*, 47 (2013) 590